Multi-Base RTK Positioning Using Virtual Reference Stations

Ulrich Vollath, Alois Buecherl, Herbert Landau, Christian Pagels, Bernhard Wagner

Spectra Precision Terrasat GmbH

BIOGRAPHY

Alois Buecherl received a degree in Computer Science at the FH Regensburg in 1994 and a Master of Science Degree in Computer Science and Engineering at the University of Connecticut in 1995. Since 1995 he is working as development engineer at Spectra Precision Terrasat, a company that actively works in the area of high-precision differential GPS since several years. Currently he is active in the area of Virtual Reference Stations.

Dr. Herbert Landau is Managing Director of Spectra Precision Terrasat. He has many years of experience in GPS and has been involved in a large variety of GPS and GLONASS developments for high precision positioning systems and applications.

Christian Pagels has a degree in Physics from the University of Erlangen (1993). He is Senior Development Engineer at Spectra Precision Terrasat and working on the design of reference station systems.

Dr. Ulrich Vollath received a Ph.D. in Computer Science from the Munich University of Technology (TUM) in 1993. He is Senior Manager of the department of kinematic positioning and real-time systems of Spectra Precision Terrasat.

Bernhard Wagner has a degree in computer science from the University of Paderborn (1993). He is working at Spectra Precision Terrasat as development engineer on the implementation of GPS and GLONASS reference stations.

ABSTRACT

In the recent past, multiple approaches have been proposed to implement the benefits of using multiple reference stations for centimeter-level accurate GNSS positioning.

A very promising and practically approved variant is the use of the Virtual Reference Station concept. Here, the modeling of error sources and the information fusion of all reference data are done centrally in a network computation center. The user is provided with Virtual Reference Station data acting like a normal local reference station. No modification of the user GPS receiver is required to use this approach opposing to other multi-base algorithms. This includes no additional requirements on the processing power of the user equipment. Another key advantage is the use of externally provided information like predicted ephemeris.

Virtual Reference Stations lead to substantial improvements for real-time positioning by reducing atmospheric, orbital and multipath errors resulting in a performance for long baseline as experienced from short baselines using only one reference station.

The paper presents the techniques necessary to process the data from the different reference stations in the network, to resolve the ambiguities inside the network and to generate the error models needed for Virtual Reference Station generation. This covers the main error sources in satellite navigation: ionosphere, troposphere, satellite orbit errors and multipath.

Fundamental limitations of ambiguity resolution in real-time, even on a network with known reference station coordinates, are presented. They impact the design and layout of a reference station network for high-precision applications.

Another paper in this publication "*Long-Range RTK Positioning Using Virtual Reference Stations*" presents practical user experiences from several operating Virtual Reference Station networks, providing fast and reliable initializations even in times of high solar activity with typically less that 1 minute initialization time on 30 km baselines, while standard reference station applications can be limited to 10 km.

INTRODUCTION

Differential GPS is a well-established technique to improve the positioning precision since many years. This

allows even centimeter-level accurate positioning using the so-called integer ambiguity resolution technique.

The basic concept is to mitigate the main error sources, ionospheric and tropospheric delay, orbit errors and satellite clock errors (where we had S/A effects, too until recently) by receiving satellite data at a well-known location. All common errors between this reference receiver and the user receiver cancel out. Though this already works quite well for many applications, the special de-correlation (i.e. the change of the errors when moving away from the reference station) of the errors leaves large error contributions in the corrected signals.

A new concept addresses this problem. The idea is to generate Virtual Reference Stations (VRS) that simulate a local reference station near by the user receiver. Thus, the errors cancel out better than by using a more distant reference station.

Integrating the data of a whole network of reference receivers, precise models of the error sources are derived. They are used to interpolate the expected errors at the user location, thus simulating a near reference receiver.

REFERENCE STATION CONFIGURATIONS

Besides Virtual Reference Station operation, operating a reference station network has multiple tasks. Following the different requirements for GPS reference station networks the operation of a network can be classified into 4 levels:

- Level 0: Station Data Integrity. This level performs analyses using the data of single stations to perform quality control / quality assurance procedures.
- Level 1: Differential Integrity. This extends level 0 to the differential observables using baselines, i.e. data from two reference stations to increase integrity.
- Level 2: Modeling of Error sources. Network-wide models for the error contributions on the positioning signals are derived in real-time to improve meter and decimeter-level positioning.
- Level 3: Virtual Reference Stations. Using the error models of level 2, the carrier phase ambiguities within the network are resolved. This is used to derive centimeter accurate measurements of the error contributions and generate a local Virtual Reference Station for the user.

The following table gives an overview of quality checks performed and stations used:

Level	Error Sources	Stations Used
0	Code chips errors (wrong code ambiguity) Coarse code outliers (tens of m) Coarse carrier phase fluctuations Cycle slips	1
1	Medium code outliers (meters) Ionospheric fluctuations Cycle slips	2
2	Long term large area errors by ionosphere, troposphere and orbits	All
3	Local errors by ionosphere, troposphere and orbits	3

Figure 1 shows the data used by each level on a sample reference station network with 4 stations.

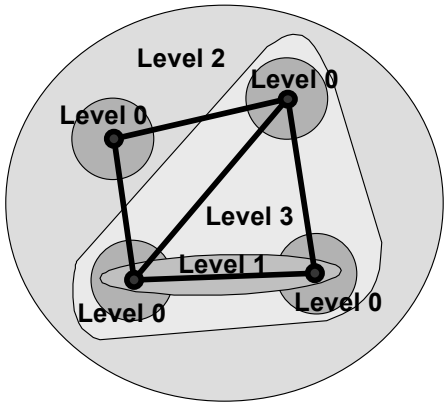

Figure 1: Level Model for Reference Station Network

Level 0: STATION DATA INTEGRITY

Station data integrity performs quality control procedures on pseudorange and carrier phase measurements. The tests are all based on the observation equations:

$$\rho_1^s(t) = R^s(t) + I^s(t) + \Delta t_r(t) - \Delta t^s(t) + T^s(t) + v_1^s(t)$$

$$\rho_2^s(t) = R^s(t) + I^s(t)\frac{\lambda_2^2}{\lambda_1^2} + \Delta t_r(t) - \Delta t^s(t) + T^s(t) + v_2^s(t)$$

$$\lambda_1 \cdot \left(\phi_1^s(t) + N_1^s\right) = R^s(t) - I^s(t) + \Delta t_r(t) - \Delta t^s(t) + T^s(t) + w_1^s(t)$$

$$\lambda_2 \cdot \left(\phi_2^s(t) + N_2^s\right) = R^s(t) - I^s(t)\cdot\frac{\lambda_2^2}{\lambda_1^2} + \Delta t_r(t) - \Delta t^s(t) + T^s(t) + w_2^s(t)$$

with

$\rho_i^s(t)$ L_i pseudorange observable of satellite s at time t

$\phi_i^s(t)$ L_i carrier phase observable of satellite s at time t

λ_i wavelength of carrier L_i

N_i^s ambiguity of carrier phase observable

$R^s(t)$ geometric range receiver to satellite s at time t

$I^s(t)$ L1 ionospheric delay for satellite s at time t

$T^s(t)$ tropospheric delay for satellite s at time t

$\Delta t_r(t)$ receiver clock error at time t

$\Delta t^s(t)$ satellite s clock error at time t

v_i^s, w_i^s measurement noise (and multipath)

For the integrity check of the pseudorange observations, a robust estimator for the receiver clock error is used to identify outliers.

The time dependent contributions ionospheric delay $I^s(t)$, tropospheric and orbit error $T^s(t)$ and receiver clock error $\Delta t_r(t)$ are estimated using carefully designed Kalman filters assuming linear time dependence:

$$I^s(t) = I_0^s + (t - t_0)\cdot I_1^s$$

The prediction of the observables for the current epoch using these filters gives a straightforward estimation of potential cycle slips on the carrier phase measurements. They can be determined using state-of-the-art integer ambiguity resolution techniques.

Level 1: DIFFERENTIAL INTEGRITY

Differential integrity inspects the single difference observables between two stations.

$\nabla\rho_i^{s,q-r}(t) = \rho_i^{s,q}(t) - \rho_i^{s,r}(t)$, etc.

Besides removing the common satellite clock error, the spatial de-correlated errors are also largely reduced. The temporal change is much smaller, too, increasing the sensibility of the tests.

As by building the single differences the information about on which station the error respective cycle slip occurred is destroyed, this is only used as additional step to assure that no compromised data is user further on. Cycle slip repair is only done in level 0.

For the differential pseudorange observations, again a robust estimator is used for approximating the differential clock error and detecting pseudorange outliers in the meter range.

Carrier phase observations are crosschecked against cycle slips that were eventually not detected in level 0 by applying triple differencing. A short-term linear behavior of the observables is assumed as before.

Level 2: MODELLING THE ERRORS

Though short-term and local effects of the atmospheric influences cannot be modeled very well – this is where the Virtual Reference Station will fit in – there are more global and long-term effects that can be predicted with a good precision using network-global error models. These models serve two purposes:

1. Provide error correction for users with less stringent requirements, i.e. DGPS users for sub-meter level positioning and "floating solution" users for decimeter precision.

2. Reduce the data present in the measurements substantially to enable network ambiguity fixing for level 3

Error contributions handled in level 2 include ionospheric errors and geometric errors, i.e. troposphere and orbit errors. Generated from the undifferenced data of all stations, it is crucial for correct performance of the system that all other error sources like cycle slip or bad tracking are identified and eliminated before generating the models.

For multipath error modeling, the repeatability of the multipath effects on a day-to-day basis can be exploited. The exact definition of this technique exceeds the scope of this paper.

IONOSPHERE ERRORS

Modeling the long term and global influence of the ionosphere on the signals is crucial for two reasons. First, this model can be used to significantly reduce the positioning error for level 2 services, improving DGPS and floating solution positioning to achieve decimeter-level positioning. Second, a reduction of the ionospheric influence is necessary to enable ambiguity fixing in level 3 (see below). The actual impact of the ionosphere on the observations can be seen in the following figures. Figure 2 shows a typical ionospheric residual during noontime in moderate latitudes (48 degree north) in December 1998, before the current solar cycle started to increase solar activity.

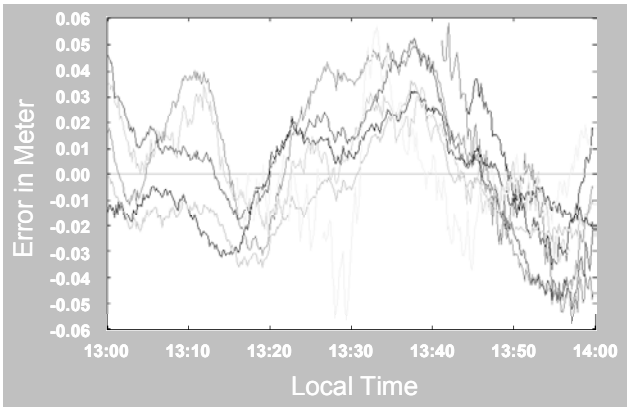

Figure 2: Noon ionosphere, December 1998

Figure 3 shows the same site at the same time of day, but now in February 2000, during a period of high solar activity. The ionospheric influence is larger by a factor of 8.

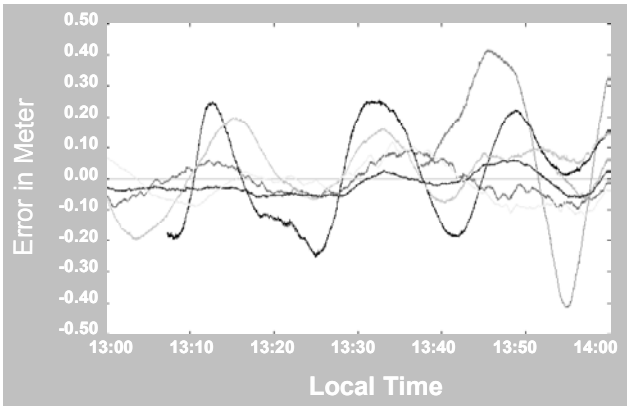

Figure 3: Noon ionosphere, February 2000

For modeling of the ionospheric delay, a single layer model of the zenith ionospheric delay was chosen. The zenith ionospheric delay is proportional to the total electron content (TEC).

The single layer models assumes that all active electron content of the atmosphere is concentrated on a layer at fixed height, e.g. 350 km. The influence of the ionosphere on the GPS signal is then computed by first computing the pierce point, i.e. the intersection point of the line-of-sight from satellite to the receiver. The zenith delay at the pierce point and the intersection angle define the ionospheric influence (Figure 4).

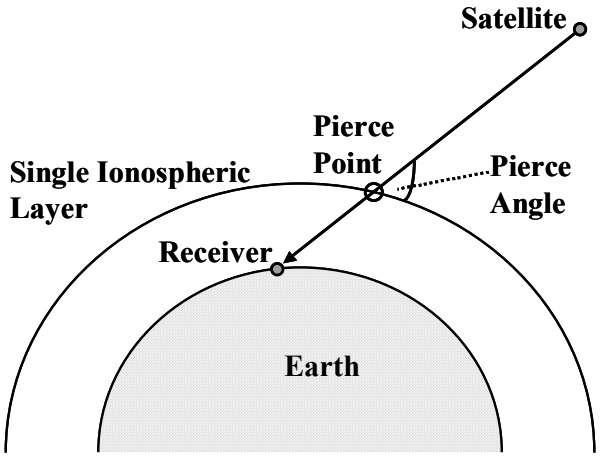

Figure 4: Single Layer Ionosphere Model

As a model for the zenith delay of the layer simple 2-dimensional polynomials over geomagnetic latitude and hour angle of the sun are used.

$$TEC(\phi_{mag},\lambda_{sun}) = \sum_{k=0}^{N} \sum_{i=0}^{k} A_{i,k} \cdot \phi_{mag}^{i} \cdot \lambda_{sun}^{k-i}$$

An order of 2 gives the best results in practice. To model temporary variations, a Kalman filter is used.

The proposed model typically removes about 50 % of the ionospheric residuals. It is especially effective for large ionospheric residuals with low temporal variations, thus reducing the impact of ionosphere in most situations. Still short-term local ionospheric effects like Transient Ionospheric Disturbances (TID) remain problematic.

TROPOSPHERE AND ORBIT ERRORS

The errors caused by the troposphere and the error in the broadcast satellite orbits are difficult to separate due to their similar characteristics: both are frequency independent and have an identical influence on pseudorange and carrier phase measurements. Nevertheless, using proper models their influences can be separated and mitigated to a certain amount.

Tropospheric errors are classically handled by using models for the zenith delay and a mapping function to

obtain the delay at a given satellite elevation angle. Unfortunately, the zenith delay depends on accurate measurements of the meteorological conditions at the receiver site. Especially for the water content of the atmosphere, the precision of hygrometers is by far not sufficient and the alternative water vapor radiometer is very expensive.

Instead, the Tropospheric scaling technique can be used with very convincing results. Here, all deviations of the atmospheric conditions from standard conditions are subsumed under a scaling factor for the zenith delay. This factor, one for each station, is the model parameter for the troposphere model. The effectiveness of tropospheric scaling can be seen in Figure 5.

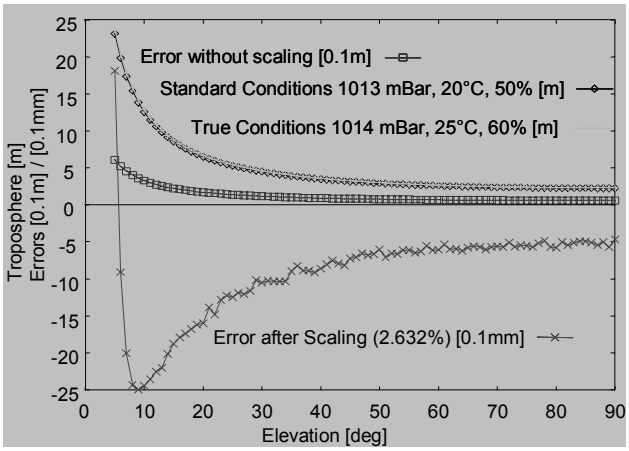

Figure 5: Tropospheric Scaling Performance

The absolute tropospheric delays, derived from a modified Hopfield model, are almost identical as seen in the two upper coinciding graphs showing a change in the meteorological conditions by 1 mBar, 5 °C and 10%. Still, the difference reaches 50 cm at low elevations, clearly compromising any centimeter-accurate ranging (middle graph). When the proper scaling is applied as shown in the lower graph, the residual error can go down to 2.5 mm even at low elevation angles.

While troposphere influences mainly low elevation satellites, orbit error have and effect that can become most prominent also on high elevation satellites. A first and very successful method is to make use of the predicted orbits supplied by the International GPS Service (IGS). These orbits are typically correct in the 50 cm range. Still, situations occur when the predicted orbits deviate from the actual positions by tens of meters.

Also, for some satellites every couple of days, no predicted orbits are available. For this reason, predicted orbits are used as primary source, but counter-checked with broadcast orbits. In the model, deviations from the predicted position are accounted for.

The influence of orbit errors and tropospheric scaling can be modeled quite easy based on the geometry of receiver and satellite.

$$\lambda_1 \cdot \left(\phi_C^s(t) + N_C^s\right) = R^s(t) + \Delta t_r(t) - \Delta t^s(t) + z_1^s(t) + TS_r \cdot TM_r^s(t) + \frac{\overrightarrow{\Delta X^s} \cdot \overrightarrow{R^s(t)}}{R^s(t)}$$

with

$\phi_C^s(t)$ ionosphere free carrier phase observable

N_C^s integer ambiguity

TS_r tropospheric scaling factor of receiver r

$TM_r^s(t)$ troposphere model value

$\overrightarrow{\Delta X^s}$ orbit error of satellite s

$\overrightarrow{R^s(t)}$ vector from satellite s to receiver

The estimated state includes the tropospheric scaling of all receivers, the orbit errors of all satellites as well as the ambiguities of the ionosphere free carrier phase combination.

Level 3: VIRTUAL REFERENCE STATION

The basic idea behind Virtual Reference Stations is to create reference station data that simulates a reference station near by the positioned receiver. This shall provide a short baseline performance to the user while removing the necessity of having an own reference receiver, preferred placed on a known point.

To apply this technique, several steps have to be performed:

1. Fixing the ambiguities of the baselines within the network allows measuring the errors on the observables with centimeter-level accuracy.

2. The data of a selected reference station, typically the one nearest to the field user, will be geometrically displaced to simulate the new position of the Virtual Reference Station.

3. The errors measured in the network are interpolated to the Virtual Reference Station location.

FIXING NETWORK AMBIGUITIES

Fixing the ambiguities inside a medium-scaled GPS reference station network can be a real challenge. Nevertheless, it is a prerequisite to centimeter-accurate determination of the error contributions on the signals in the same way as it is necessary for centimeter-level positioning.

As the ambiguities of the ionospheric and the ionosphere-free observables are already model parameters of the error models used for level 2 services, their estimates are ideally suited for ambiguity determination. They accumulate all data collected so far, and reduction by the error models is done implicitly as the error model parameters are determined. Also, the models provide the correlations between the estimated ambiguities further strengthening the ambiguity resolution.

Still, the requirements for the precision of the estimated double differences are stringent. Figure 6 shows the base 2 logarithms of the expected ratios of variance as standard criterion for successful ambiguity resolution as a function of residual error in the ionosphere ambiguity and the troposphere ambiguity.

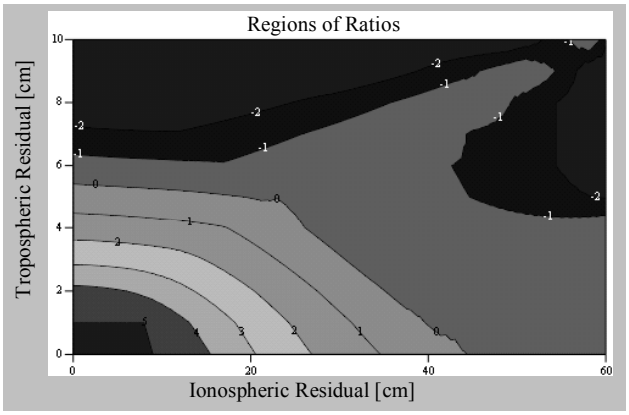

Figure 6: Ratio Regions for Network Fixes

The models must reduce the estimation errors to a level in the area of ratios above 2 (log 2 above 1) for the correct solution after a sufficient time span of data collection.

For efficient ambiguity resolution, the ambiguity estimates N_I from ionosphere model and N_C from troposphere model must be mapped back into the original N_1/N_2 domain of the integer ambiguities of the basic carrier phase observables on L1 and L2. The following relation assists in the solution of this problem:

$$\begin{pmatrix} N_C \\ N_I \end{pmatrix} = \begin{pmatrix} \alpha_1 & \alpha_2 \\ -\lambda_1 \cdot \frac{\lambda_2^2 - \lambda_1^2}{\lambda_1^2} & \lambda_2 \cdot \frac{\lambda_2^2 - \lambda_1^2}{\lambda_1^2} \end{pmatrix} \cdot \begin{pmatrix} N_1 \\ N_2 \end{pmatrix} = T \cdot \begin{pmatrix} N_1 \\ N_2 \end{pmatrix}$$

Inverting the conversion matrix T leads to the form:

$$\begin{pmatrix} N_1 \\ N_2 \end{pmatrix} = \overline{T} \cdot \begin{pmatrix} N_C \\ N_I \end{pmatrix}$$

Basic error propagation laws define the variance-covariance of the N_1/N_2 ambiguities as function of the N_C/N_I variance-covariances.

$$\sigma^2(N_1, N_2) = \overline{T} \cdot \sigma^2(N_C, N_I) \cdot \overline{T}^T$$

As the estimates of both models can be assumed to be uncorrelated with each other, this can be done for both models separately, adding the results afterwards:

$$\begin{pmatrix} N_1 \\ N_2 \end{pmatrix} = \overline{T} \cdot \begin{pmatrix} N_C \\ N_I \end{pmatrix} = \overline{T}_C \cdot N_C + \overline{T}_I \cdot N_I$$

$$\sigma^2(N_1, N_2) = \overline{T}_C \cdot \sigma^2(N_C) \cdot \overline{T}_C^{\,T} + \overline{T}_I \cdot \sigma^2(N_I) \cdot \overline{T}_I^{\,T}$$

Now, the established variance/covariance-based ambiguity resolution methods can be used to determine the best solution. After careful validation, the ambiguities can be fixed.

REFERENCE DATA DISPLACEMENT

To make the transmitted data look like it came from a different position, it has to be displaced geometrically. This means that all parts of the observation equations that depend on the receiver location have to be corrected to a new position.

For the geometric range R between satellite and receiver a special problem arises. R is defined as

$$R^s(t) = \sqrt{\left(\overrightarrow{x^s} - \overrightarrow{x_r}\right)^T \cdot \left(\overrightarrow{x^s} - \overrightarrow{x_r}\right)}$$

$\overrightarrow{x^s}$ satellite position at send time in earth-centered earth-fixed system

$\overrightarrow{x_r}$ receiver position

As the rotation of the earth during transit of the signal from the satellite to the receiver has to be accounted for, and the signal transit time changes due to the change in the receiver position, the following approach is used. Let $\overrightarrow{x_r}$ be the position of the original reference station and $\overrightarrow{x_v}$ the position of the Virtual Reference Station. A first approximation of the new geometric ranges is

$$\tilde{R}_v^s = \sqrt{\left(\overrightarrow{x^s} - \overrightarrow{x_v}\right)^T \cdot \left(\overrightarrow{x^s} - \overrightarrow{x_v}\right)}.$$

Due to the uncorrected satellite position it is accurate only in the meter range. Using this range approximation, a pseudorange can be generated for the new position, also accurate in the meter range:

$$\tilde{\rho}_v^s = \rho_r^s + \left(\tilde{R}_v^s - R_r^s\right).$$

This pseudorange approximation now is sufficient to determine the exact satellite position with the standard algorithms for orbit evaluation and earth rotation. Derived from this, the exact geometric range R_v^s is available. The change in the geometric range $\Delta R^s = R_v^s - R_r^s$ can be applied to all observables to displace the measurements to the new virtual position.

ERROR INTERPOLATION

When interpolating the errors for the Virtual Reference Station, a change in the error models used occurs. While level 2 services used network-global models, now linear 2-dimensional models are used. For this, the reference station network is triangulated. To interpolate to a specified position, the triangle including this position is chosen. It is also possible to extrapolate outside the reference station network using the same techniques (Figure 7).

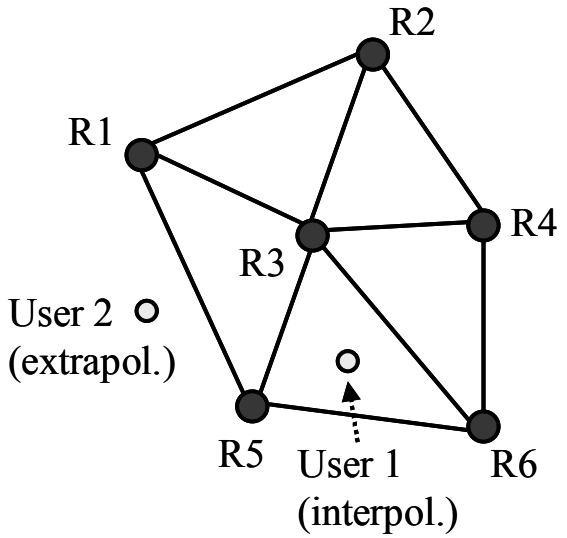

Figure 7: Interpolation and Extrapolation

Now, the differential errors between the 3 stations of the triangle selected are used to set up a linear model. Carrier phase measurements on ionosphere on the ionospheric-free combination are handled separately. One station of a triangle is selected as pivotal station, with coordinates (ϕ_r, λ_r). Now the double differences between the station can be interpolated with the formula:

$$\Delta\nabla_C(\phi,\lambda) = P_{C,N} \cdot (\phi - \phi_r) + P_{C,E} \cdot (\lambda - \lambda_r) \cdot \cos\phi_r$$

Given the double differences to the other two triangle stations (ϕ_1, λ_1) and (ϕ_2, λ_2), the interpolation parameters $P_{C,N}$ for the north direction and $P_{C,E}$ for east are defined by the equation:

$$\Delta\nabla_C(\phi_1,\lambda_1) = P_{C,N} \cdot (\phi_1 - \phi_r) + P_{C,E} \cdot (\lambda_1 - \lambda_r) \cdot \cos\phi_r$$
$$\Delta\nabla_C(\phi_2,\lambda_1) = P_{C,N} \cdot (\phi_2 - \phi_r) + P_{C,E} \cdot (\lambda_2 - \lambda_r) \cdot \cos\phi_r$$

To interpolate or extrapolate, the formula above is applied to the Virtual Reference Station coordinates (ϕ_v, λ_v).

The performance of this generated Virtual Reference Station depends on the actual linearity of the errors over space. Figure 8 illustrates the situation:

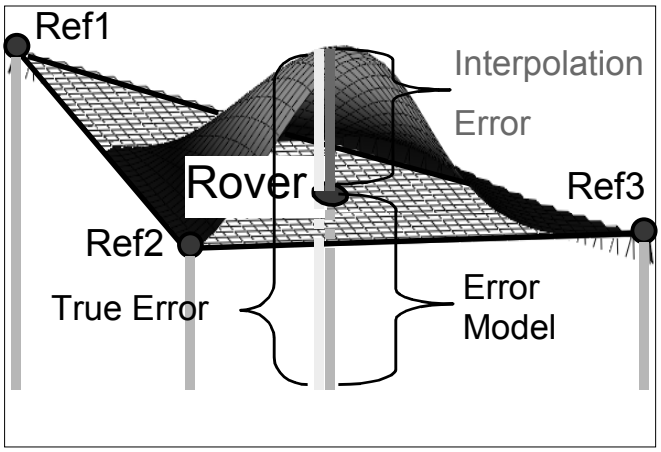

Figure 8: Linear Interpolation Error

The triangular plane represents the linear error model exactly interpolating the measured errors at the three stations. A rover placed inside the triangle will get a Virtual Reference Station with the interpolated errors generated (Error Model). The real error (True Error) can deviate from linearity, here shown exaggerated as the bended surface. The difference between the plane and the real error will remain in the differential positioning of the rover with the Virtual Reference Station (Interpolation Error).

TYPICAL FIELD SET-UP PROCEDURE

On a typical field session, the following set-up procedure is performed (Figure 9).

1. After starting the local receiver in real-time positioning mode, the user dials into the Virtual Reference Station Network service via a mobile phone capable of data transmission. This is normally done using one central phone number available for a whole state or country.

2. When the caller is successfully authenticated, the local receiver sends a navigation solution of its current position as a rough position estimate to the computing center.

3. After receiving the rough position estimate, the computing center creates a Virtual Reference Station at this location.

4. A continuous data stream of reference data generated for the Virtual Reference Station position is sent to the field user receiver. This can be done in RTCM or other real-time formats like CMR2.

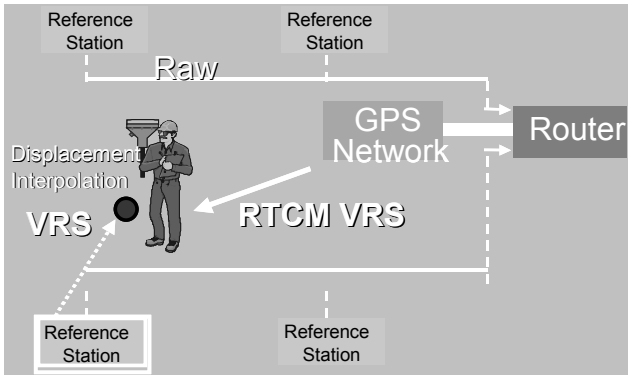

Figure 9: VRS Field Set-Up

On networks where a dial-in via mobile phone services is not practicable due to availability or cost reasons, broadcast services are alternatively used. Here, the reference data of one or more stations are broadcast together with the error model parameters using dedicated or existing radio transmitter stations. This requires additional efforts at the receiver side. To support this technique, a common standard for broadcasting network corrections would be beneficial. An extension to the upcoming RTCM 3 standard could help to enable network corrections in a standard way implemented on all major receivers.

OPERATING REFERENCE STATION NETWORKS

The presented concepts are implemented in a number of reference station network installations since up to 2 years. Many experiences about operation and performance could be collected. The following table gives an overview of some existing installations of Virtual Reference Station Networks by our company.

Network	Location	Stations
ByS@t	S.Germany	9
SAPOS	S.Germany	15
Ruhrgas	Germany	7
SwissS@t	Switzerland	21
Swiss Topo	Switzerland	22
Bay Area Network	California	4
Geoditech	Finland	3
SWEPOS	Sweden	5

PERFORMANCE RESULTS

Using a network with a reference station separation of about 70 km, performance analyses were done comparing a standard RTK system receiving only data from one reference station with an RTK system receiving Virtual Reference Station data from the network.

The distance from the rover to the nearest reference station was 32 km. The rover setup included a high multipath environment, leading to over-average times to fix. Data was collected in week 36, Sep. 2000, during high solar activity. The full analysis is topic of another paper in this publication. Here we just present Figure 10 as an overview of the performance gain.

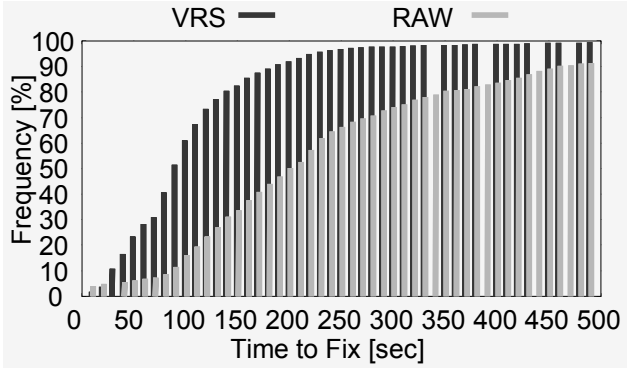

Figure 10: Times to Fix, VRS/Raw

Figure 10 shows accumulated times to fix, e.g. a value of 90 seconds at 50 % frequency for VRS means that 50 %

of the fixes were faster that 90 seconds. Using VRS could significantly reduce initialization times with OTF by a factor of 2.

CONCLUSIONS

The Virtual Reference Station technique has proven its performance in several existing networks. The major benefits vs. use of classical reference stations are:

- Improvement of accuracy versus classical RTK for DGPS, decimeter-level and centimeter-level positioning.
- Reliability improvement by increased integrity of the transmitted signals and better performance of ambiguity resolution due to smaller biases.
- Productivity improvement by shortening the convergence time of ambiguity resolution.
- Local reference station is obsolete as appropriate reference data is generated by the computing center on dial-in.
- Positions are automatically derived in a precise geodetic reference station system.
- Additional real-time services for ionospheric disturbances can be provided to the user.

Using a system of 4 levels of reference station network operation, the system provides the optimal functionality for the reference station network operator.

REFERENCES

[1] Wild, U., Beutler, G., Gurtner, W. and Rothacher, M: *Estimating the Ionosphere using One or More Dual Frequency GPS Receivers.* Proceedings of the 5th International Geodetic Symposium on Satellite Positioning, Las Cruces, New Mexico, March 13-17, 1989.

[2] Sjöberg, L: The Best Linear Combination of L1 and L2 Frequency Observables in the Application of Transit/Doppler and GPS, manuscripta Geodetica 15 (1990), p. 17-11.

[3] Beutler, G., Schaer, S. and Rothacher, M.: *Wide Area Differential GPS, Study in the Context of AGNES*. Printing Office, University of Bern, September 17, 1999

[4] Collins, J.P. and Langley, R.B.: *Possible Weighting Schemes for GPS Carrier Phase Observations in the Presence of Multipath*, Geodetic Research Laboratory, Department of Geodesy and Geomatics Engineering, University of New Brunswick, Canada. For United States Army Corps of Engineers Topographic Engineering Center, March 1999.

[5] Jonge de, P.J., and C.C.J.M. Tiberius (1996) Integer ambiguity estimation with the LAMBDA method. *Proceedings IAG Symposium No. 115, GPS trends in precise terrestrial, airborne and space borne applications,* XXI General Assembly of IUGG, July 2-14, Boulder, CO, July 2-14, 1995, G. Beutler et.al., (Eds.), Springer Verlag, pp. 280-284.

[6] Jonge de, P.J., and C.C.J.M. Tiberius (1996) The LAMBDA method for integer ambiguity estimation: implementation aspects. *Delft Geodetic Computing Center LGR series,* No. 12.

[7] Vollath, U., Buecherl, A., Landau, H. Pagels, C., Wagner, B.: "Long Range RTK Positioning using Virtual Reference Stations", *To be published in proceedings of the ION GPS 2000.*